



Contents lists available at *Dergipark*

## Journal of Scientific Reports-A

journal homepage: <https://dergipark.org.tr/pub/jsr-a>



**E-ISSN: 2687-6167**

**Number 55, December 2023**

### **RESEARCH ARTICLE**

Receive Date: 17.04.2023

Accepted Date: 30.10.2023

# Rapid processes for the production of nanocrystal yttria-stabilized tetragonal zirconia polycrystalline ceramics: ultrasonic spray pyrolysis synthesis and high-frequency induction sintering

Muhterem Koç<sup>1\*</sup>, Osman Şan<sup>2</sup>

<sup>1\*</sup>Kütahya Dumlupınar University, Department of Industrial Design, Kütahya, 43100, Turkey. ORCID: 0000-0003-3661-4410

<sup>2</sup>Kütahya Dumlupınar University, Department of Materials Science and Engineering, Kütahya, 43100, Turkey, ORCID: 0000-0001-6033-5804

## **Abstract**

In this study, nanocrystalline 3 mol % yttria-stabilized tetragonal zirconia polycrystalline (Y-TZP) ceramic was produced by sintering with a high-frequency induction heating (HFIH) system of granular powders obtained by ultrasonic spray pyrolysis (USP) at 600 °C. The granular nano-sized powders (10-30 nm) were micron in size (average size: 700 nm), spherical in shape and amorphous. The influences of the HFIH sintering temperature (1400-1600 °C), applied current time (60-300 sec.) and the mechanical pressure (10 MPa and 20 MPa) on the final density and grain size of the products were investigated. The amorphous granular Y-TZP powders compressed with the HFIH system allow very rapid condensation in the tetragonal phase at high density and avoid grain growth. High density (relative density over 95) nanocrystalline Y-TZP ceramic with ~70 nm size could be obtained from the simultaneous application of 20 MPa pressure and an induced current within 300 sec. of sintering time at 1500 °C. In this condition, the sample's maximum hardness and fracture toughness values were reached at 14.9 GPa and 3.8 MPa·m<sup>1/2</sup>, respectively. Y-TZP powders produced in nano-micro structure with the USP system were sintered with the HFIH system and rapid production was achieved by preventing grain growth.

© 2023 DPU All rights reserved.

*Keywords: Granular powder, Y-TZP, rapid processes, microstructure.*

\* Corresponding author. Tel.: +90 (274) 443 44 61

E-mail address: muhterem.koc@dpu.edu.tr

<https://orcid.org/0000-0003-3661-4410>

## 1. Introduction

The zirconia based ceramic materials has been widely used in modern technologies because of the unique combination of physicochemical properties such as mechanical strength, hardness, toughness, refractory properties as well as the high resistance to aggressive media. The performance of zirconia material increased by the stabilization as tetragonal phase using some additives such as  $Y_2O_3$ , CaO,  $CeO_2$ , MgO, etc. [1–4]. The use of 3 mol% yttria was main additive and it was proved that the zirconia ceramic has excellent strength and toughness [5]. Moreover, the study of Wakai et al. [6] revealed that when yttria- stabilized zirconia ceramics have been produced, they have exhibited superplastic properties.

The superplastic deformation behavior of the yttria-stabilized tetragonal zirconia is primarily dependent on small grain sizes [7–9]. However, it is difficult to obtain the grains which are smaller than 100 nm in size. The conventional pressureless sintering required a high temperature and long-time sintering for sufficient densification and thus this condition leads to grain growth phenomenon by diffusion. Therefore, it is necessary to analyze the fabrication of zirconia ceramics such as hot pressing [10,11], spark plasma sintering [12], hot isostatic press [13,14], high frequency induction sintering [15–18]. In these processes, the applied pressure has great importance on the rearrangement of the particles during the compaction as well as the densification. The powder compaction not only depends on the applied pressure, but also the nature of thermal environment, the size, the size distribution, and the shape of the particles greatly determine the densities [19,20]. However, the research was focused on the effect of applied pressure on the densification which were correlated by the grain growth to find optimum conditions [21,22].

It is known that the densification of ceramics is achieved by two mechanisms: (i) the shrinkage of the open pores and (ii) the grain boundary diffusion. In the conventional pressureless sintering, the transition from the open pore structure to the closed pore takes over a long period of time. In this process, the grain growth is low, in which the pores repress the grain growth. The main grain growth is seen during the process where the open porous structure disappears. At this stage, high mass transport occurs with diffusion by increasing intergranular contact. In sintering under pressure, the two processes are quick and the period in which the high packing process is penetrated is of even greater importance. In this way, the mass transport takes place at high level and the grain growth increases rapidly. Therefore, in the sintering processes under pressure, the relationship between the duration of sintering and the grain growth must be carefully determined. This process can lead to high grain growth in a much shorter period of time depending largely on the applied pressure [21]. Recently, forming of a second phase at the grain boundary or grain boundary precipitation to control of grain growth in sintering process has been studied. [23,24]. However, the thing that shouldn't be forgotten here is that the primary properties of the starting powder are much more effective. The subject matter which is more important than producing second phase is morphology of the powders, deformation ability, porosity and porosity distribution and homogeneous phase structure control.

In order to obtain yttria stabilized zirconia nanocrystalline ceramic, some methods such as co-precipitation [25], sol-gel technique [26] and USP system [27] have been employed to prepare the starting nano powders. There are two basic process difficulties in material production from nano-sized powders. First, the fine powders show rapid aggregation in the production process which makes high density packing impossible. Secondly, the nano-powders rapidly form grain growth at high temperatures, therefore, the preparation of the nano-sized starting powders cannot contribute positively to the physical properties of the produced material. Recently, intense efforts have been made to process nano-sized powders. The most remarkable method in this area is the production of nano-powders as agglomerate granules. The USP system seems to be quite successful in establishing these controlled agglomeration conditions. Particularly, easy controllable parameters such as the composition of the solution to be fed into the system, surface energy and reactor temperature allow agglomerated powder production with different properties. In this system, the initial stoichiometry in the produced powders is preserved on grain basis, and agglomerations of primary crystals and the micro-spherical particles composed of nano-sized particles can be produced as porous or dense structure depending on the reactor temperature [19]. Kang et al. [25] synthesized hollow Y-TZP powders (600 and 900 °C) and transformed them into nano-scale particles by planetary milling. As a result of the conventional sintering process (1300-1500 °C), these powders were found to be below 1 µm at 1300 and 1400 °C and 2.3 µm due

to the grain growth at 1500 °C. The sintering of these powders under pressure with fast sintering is expected to provide higher performance. On the other hand, no literature has been found on the sintering of Y-TZP powders produced by the USP system directly (without the milling process) under pressure with HFIH method.

In our present work, the Y-TZP nanocrystalline ceramics were fabricated by the rapid processes such as HFIH of the granule powder obtained by USP system. The granule powder was obtained from yttrium and zirconium hydroxide colloidal solution at the reactor temperature of 600 °C. The effects of the sintering temperature (1400-1600 °C) for different holding times (60-300 sec.) on the relative density, average grain size, phase microstructure, and vickers micro hardness of the Y-TZP nanocrystalline ceramics were investigated.

## 2. Materials and Methods

The Y-TZP granular particles were prepared by the USP technique using an ultrasonic nebulizer. Zirconium (IV) nitrate hydrate ( $\text{ZrO}(\text{NO}_3)_2 \cdot 6\text{H}_2\text{O}$ ) (99 %,Sigma), yttrium (III) nitrate hydrate ( $\text{Y}(\text{NO}_3)_3 \cdot 6\text{H}_2\text{O}$ ) (%99.8,Sigma), ammonium hydroxide solution ( $\text{NH}_4\text{OH}$ ) (30-32%, Sigma) and nitric acid  $\text{HNO}_3$  (70%, Sigma) were selected as starting materials. The synthesis of  $\text{ZrO}_2\text{-Y}_2\text{O}_3$  solution was carried out by co-precipitation method. Precursor solution of 0.97 mol  $\text{ZrO}_2$  and 0.03 mol  $\text{Y}_2\text{O}_3$  were prepared by dissolving in deionized water and mixed using magnetic stirrer at 500 rpm until obtaining a clear solution. Then, the  $\text{NH}_4\text{OH}$  solution was added dropwise into a continuously stirred precursor solution (pH~9) and subsequently the mixture was filtered for the removal of precipitate. The precipitate was washed three times with deionized water in order to ensure that the  $\text{NO}_3$  and  $\text{NH}_4\text{OH}$  was completely removed from the precipitate. Yttrium and zirconium hydroxide colloidal sol solution was adjusted to pH 3 using nitric acid. Then the Y-TZP particles were produced with the ultrasonic spray pyrolysis (USP) system at 600 °C reactor temperature. The overall concentration of zirconium and yttrium sources was fixed at 0.1 M in deionized water and ethanol (water/ethanol ~3). The frequency of the ultrasonic nebulizer and the feed rate of the carrier gas were 1.63 MHz and 2 Lt/min, respectively. Quartz tube with a length of 120 cm and a width of 5 cm was used for powder production. The powders produced from the USP system were collected in three gas washing bottles connected in series at the outlet. The details of the ultrasonic spray pyrolysis system were given elsewhere [28].

In the sintering process of powders, a HFIH system with a frequency of 900 kHz and a power of 2.5 kW was used. The sintering process was carried out at different dwelling times (60-300 sec.) between 1400 and 1600 °C. Powder sintering was performed in a vacuum tank, under pressure and with the help of graphite mould. The powders were placed in the system by being filled in a graphite mould (outer diameter: 20 mm, inner diameter: 10 mm and height: 20 mm) and were pressed under pressure of 10 and 20 MPa during the sintering process with the help of a uniaxial pressing. The heating rate was over 1000 °C/min and the temperature was measured on graphite mould by optical pyrometer (600-2200 °C). Sintering process consisted of the following steps: (i) firstly a vacuum of 30 mTorr was applied to the system, (ii) the powder in the graphite mould was compressed with uniaxial pressing (iii) the sintering process started by activating the induction system, (iv) when the sintering process finished, it was allowed to cool down to the room temperature, the vacuum was closed, the pressure was removed, and the sample was taken out of the mould.

Thermal decomposition behavior of USP powder was determined by TG-TGA analysis (Perkin Elmer–Diamond) up to 1500 °C at heating rate of 10 °/min. The phases of the prepared powder and samples were determined by XRD (Rigaku-MiniFlex) analysis. XRD analyses were performed at a speed of 2°/min with 0.01° steps using  $\text{CuK}\alpha$  radiation between 20° and 80°. The crystal size of Y-TZP bulk materials was calculated by Scherrer formulation applied to XRD analysis. The density of the samples was determined by the method of Archimedes. The morphology of the powders and the samples were determined by the scanning electron micrographs (SEM) (Zeiss Supra 50 VP) (Bulk samples were polished and investigated by performing platinum plating on surfaces that were thermally etched at 1250 °C). Particle size distribution was determined by SEM image (using Image J software) and Malvern/Mastersizer 3000. The structure of the particles was characterized by TEM (JEOL JEM 2100F HRTEM). The Vickers microhardness and fracture toughness values of the materials were measured by the notch marks made under 1 kg of force applied for 15 seconds (Duraline M Mikro-Vickers). At least five measurements were taken for

each sample. The fracture toughness was calculated from the crack length under load.

### 3. Results and Discussion

#### 3.1. Properties of USP granule particles

Fig. 1a-d shows the physical characteristics of the Y-TZP granule powders through the analysis of XRD phase (a), particle size distribution (b), SEM microstructure (c), TEM (d). The obtained results are as follows: (i) it was found that that the granule powder in amorphous structure could be obtained with the low reactor temperature (600 °C) (Fig. 1-a), (ii) the size distribution of the granules was suitable for high density packaging; the average size of the powders was  $\approx$ 700 nm and showed a monomodal distribution between 118 nm and 2099 nm (Fig. 1-b), (iii) the granules preserved sufficient spherical structure, there was no primary particles (Fig. 1-c), (iv) micro-sized granules were composed of the primary particles where the grains were in nano-sizes (10-30 nm) (Fig. 1-d).

In the present study, the appropriate reactor temperature was firstly determined. As known, the amorphous powders show high sintering properties and thus the reactor temperature was adjusted to obtain the granule powder in amorphous phase; the applied reactor temperature of 600 °C did not lead to crystallization. On the other hand, the powders must be granule grains, so the temperature should be sufficient to improve the agglomeration. Perez–Page et al. investigated yttria stabilized zirconia powders with the USP system for temperatures between 700 °C and 1200 °C and revealed that these powders were crystallized at 700 °C temperature and the crystallization increased depending on the increase in reactor temperature [29]. In our present study, the selected reactor temperature was relatively low. Powder produced at 600 °C was amorphous with the spherical granules in micron size. The powder was expected to be densify by the induction sintering process under the target pressure, which will provide high density packing with low grain growth.

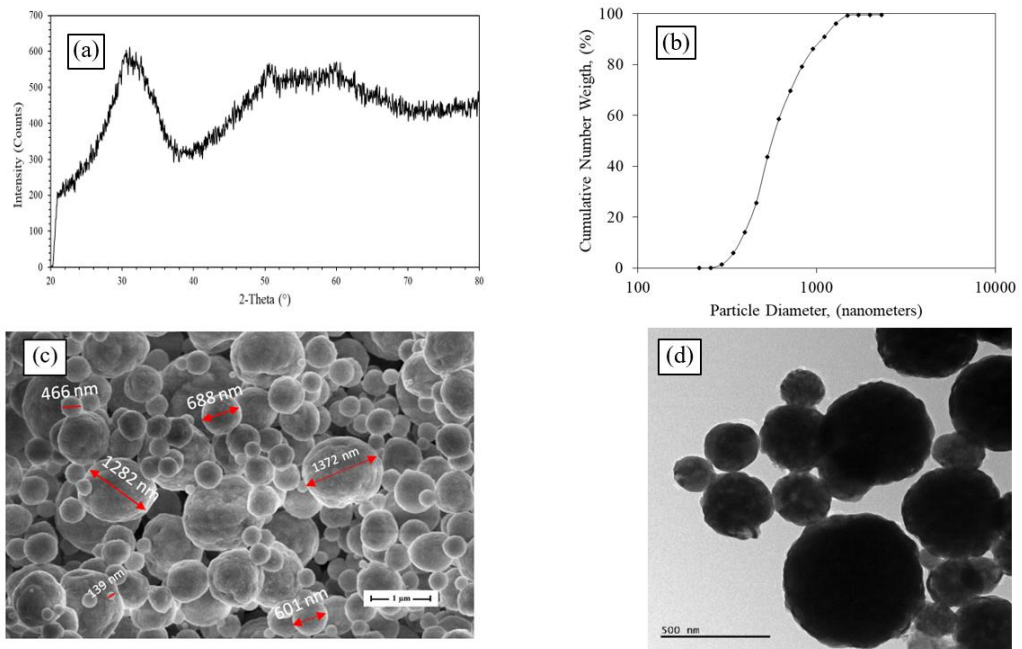


**Fig. 1.** The characterization of Y-TZP granule powder obtained by USP system: (a) XRD analysis, (b) particle size distribution, (c) SEM image, (d) TEM analysis.

### 3.2. High frequency induction heating sintering

Sinterability of the amorphous spherical Y-TZP granule powders by HFIH method was investigated for two different pressure values. When the pressure value was at 10 MPa and the sintering temperature was in between 1400 and 1500 °C and the sintering time was 300 s, the grain size of the material obtained was in between 200 and 250 nm. In this process, there were voids within the microstructures (Fig. 2) and the grain growth was low. When the sintering temperature was 1600 °C, it was observed that the relative density was reached to a great extent (> 96%) but the uncontrolled growth of the grains occurred, and these grains had average size of 2-5 µm. Here, the increase in grain growth may not be the only reason for the high sintering temperature. It is known that the soaking time during the sintering process has a great effect on the characteristics of the grain. Therefore, during the sintering process at 1600°C where grain growth occurred, the dwelling time was reduced to 60 sec. In this short sintering process, the density of 98% was provided, but the grain growth was still high and extremely irregular; there were grains with 200 nm size as well as up to 2 µm (Fig. 3). Grain growth could not be prevented by the sintering process performed under these conditions. Therefore, pressing pressure was increased in order to be able to achieve packing at lower temperatures to prevent the grain growth.

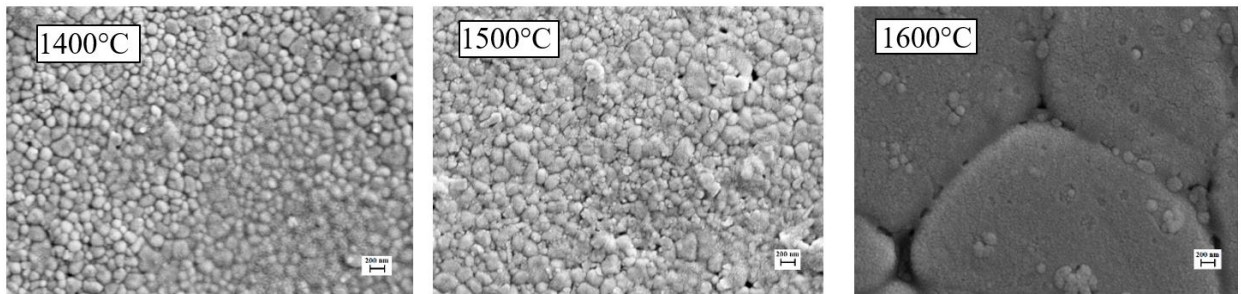


**Fig. 2.** Microstructures of samples sintered at different temperatures for 300 sec. at a pressure of 10 MPa.

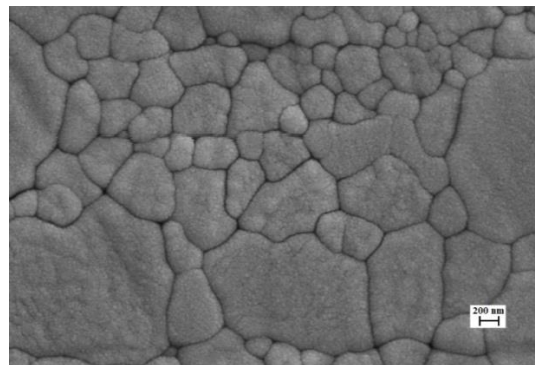


**Fig. 3.** Microstructure of samples sintered at 1600 °C for 60 sec. under pressure of 10 MPa.

When the pressure was 20 MPa, grain growth in the samples obtained as a result of sintering for 300 seconds at 1400-1500 °C was within the acceptable limits (<500 nm). While the material density of the sample with a sintering

temperature of 1400 °C was 92%, this value was 95% at 1500 °C. When the sintering temperature was 1600 °C (Fig. 4), it was seen that the grain growth increased, and the average grain size was found to be 5 µm. Therefore, when density and grain growth results were evaluated, the product with 95% density with a dwelling time of 300 seconds at 1500°C gave the best results. In this case, the grain size was below approximately 500 nm and there was a uniform grain size distribution (Fig. 4). Fig. 5 shows the XRD analysis of the samples sintered at 1400-1600 °C. The materials successfully crystallized into the tetragonal zirconia phase during the short-term sintering process (Fig. 5). The crystal size of the sample produced at 1500 °C with high density and low grain growth is approximately 73 nm. This value was also similar to the low temperature sintered (1400 °C) powders (about 71 nm). However, this value increased with sintering at high temperature (1600 °C) and reached up to 88 nm. An increase in crystal size increased the grain growth at high level. Therefore, in this study, the sintering temperature was determined as 1500 °C for low-grain growth and high-density material production.

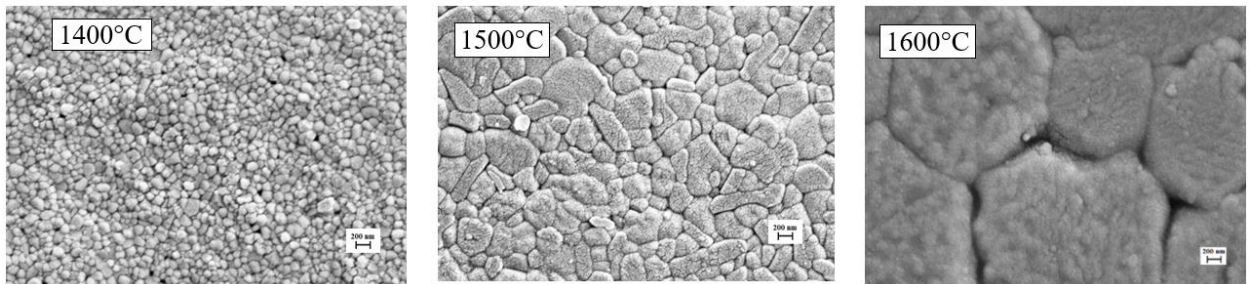


**Fig. 4.** Microstructures of samples sintered at different temperatures for 300 sec. at a pressure of 20 MPa.

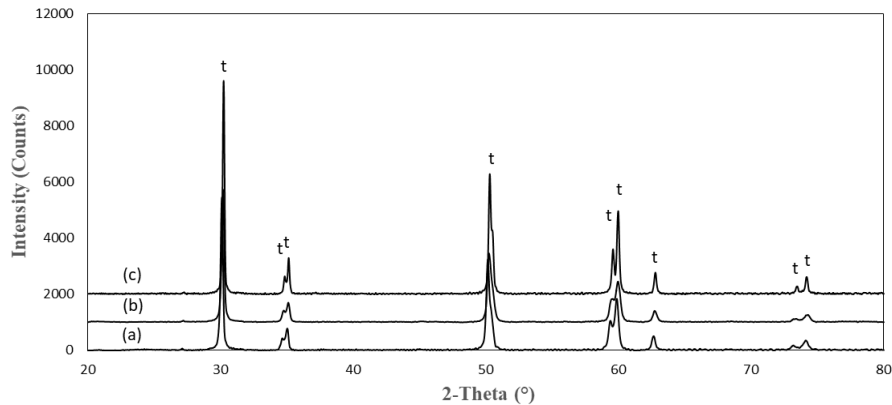


**Fig. 5.** XRD patterns of samples sintered at 1400-1600°C for 300 sec. under 20 MPa pressure; (a) 1400 °C, (b) 1500 °C, (c) 1600 °C (t: tetragonal phase).

### 3.3. Mechanical performance

The mechanical performances of Y-TZP ceramics obtained in this study were examined with the hardness and toughness measurements carried out for 15 seconds under a load of 1 kgf in polished surfaces. The hardness

performance of the samples with low pressure processing was also low (Fig. 6). The hardness values of the samples prepared at high pressure (20 MPa) increased, with increasing density values (Fig. 7). The highest hardness value was determined to be 14.9 GPa for the sample sintered at 1500 °C under pressure of 20 MPa for 300 sec. At 1600 °C, the hardness value of the samples decreased, and the density was still high (see Fig. 7). This decrease in hardness was associated with grain growth. Fig. 8 indicates the cracks under load. Toughness values were calculated by using crack size according to the equation of Anstis [30] and the toughness values were found to be 3.2-3.8 MPa.  $M^{1/2}$ . In the HFIH system, this value for the sample which was sintered at 1500 °C under 20 MPa pressure for 300 sec. was calculated to be 3.8 MPa  $M^{1/2}$ . The fracture toughness result of the sintered 3-5 mol%  $Y_2O_3$  stabilized zirconia specimen is quite compatible with the literature [31].

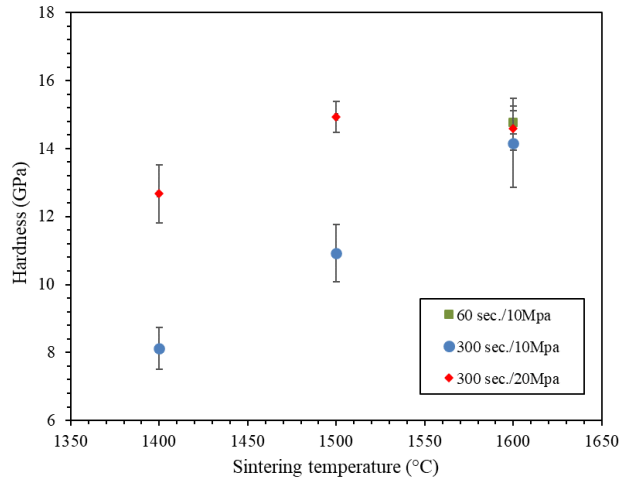


**Fig. 6.** Hardness of samples sintered at different temperatures.

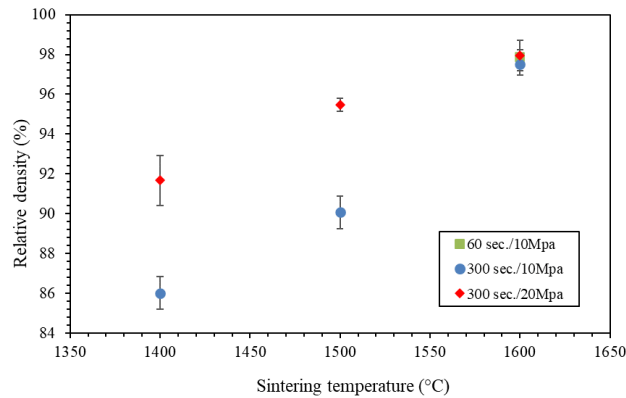


**Fig. 7.** Relative density of samples sintered at different temperatures.

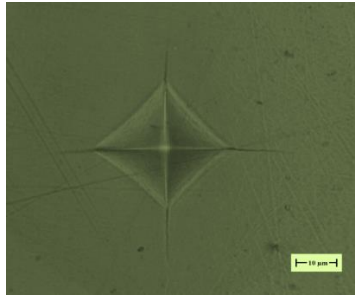


**Fig. 8.** Optic photographs of the Vickers indentation in the sample sintered at 1500°C for 300 sec under pressure of 20 MPa for fracture toughness evaluation.

The sinterability of amorphous granules obtained through USP system under pressure with HFIH was schematically illustrated in Fig. 9a-c. The phases of this process were as follows: (i) the cold packaging of the powders under pressure indicated loose compaction (Fig. 9-a) (ii) the pressure with applied temperature led to shrinkage and disintegration of the agglomerates as well as the transformation of amorphous powders into oxide form (Fig. 9-b) (iii) the densification and crystallization stage (Fig. 9-c). It is useful to draw attention to the following; initially the granules had high compaction and later in the second stage they were collapsed in the mould and dispersed without any change in their initial positions; the positions of the spherical granules can be distinguished from Fig 9-b.

Fig. 10 shows the TG analysis of Y-TZP powders with a total weight loss of 16.24%. This weight loss was due to the -OH groups driven away because of the conversion of zirconium hydroxide into oxide form. Under the influence of pressure and temperature, the granules became extremely smaller due to the conversion mentioned above. Thus, the granules became loose and were compacted in nano size. This process played an important role in packing of the granules. At the end of this process, a structure of high density and homogeneous distribution was obtained.

As the sintering process continued, condensation increased and grain growth in the samples remained limited. It is thought that the powders produced by the USP system were initially amorphous. Crystallizations coexisted with the deformation process suppressing the grain growth. Thus, products of low-grain growth and high-density with a homogeneous microstructure were obtained. In sintering with the HFIH heating system, the amorphous powders obtained by USP system were found to be of great importance in terms of preventing the grain growth.



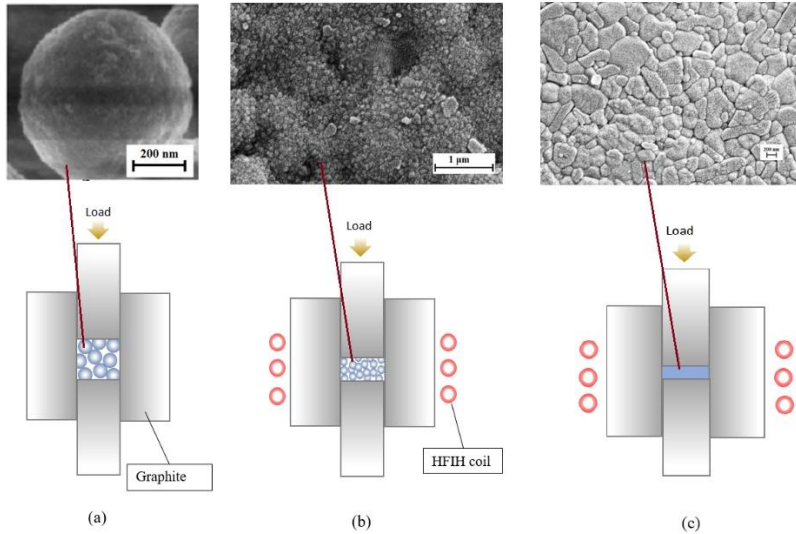


**Fig. 9.** The mechanism of sintering of the powders produced by the USP system with the HFIH system, a) before sintering, b) sintering at 1400 °C under 20 MPa pressure for 60 sec. c) sintering at 1500 °C under 20 MPa pressure for 300 sec.

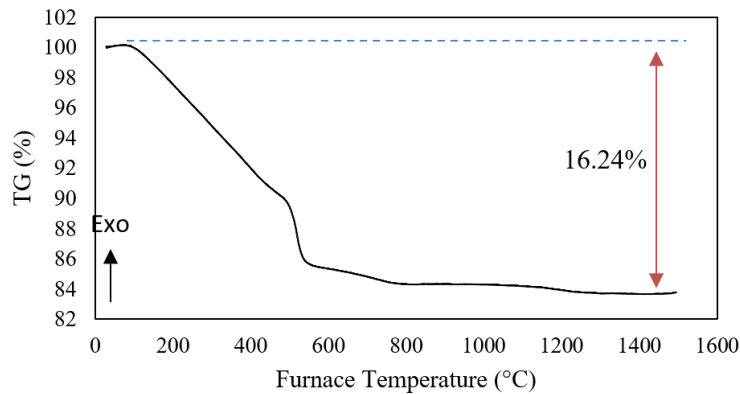


**Fig. 10.** TG analysis of Y-TZP powders produced by USP system.

#### 4. Conclusions

In this study, amorphous Y-TZP powders were obtained by USP system, which is a rapid powder production process, at 600 °C in a nano-structured spherical shape. These powders were successfully sintered (fast sintering) with HFIH system. The granule particles having average size of  $\square$ 700 nm were obtained from the primary particles of 10-30 nm in size. It was determined that these powders crystallized in the tetragonal zirconia phase as a result of sintering at high temperatures (1400-1600 °C) and the crystal size increased from 71 nm to 88 nm depending on the sintering temperature. Grain growth occurred in powders exposed to high temperatures for high density at low

pressure. Y-TZP powders were sintered at 1500 °C under 20 MPa pressure for 300 seconds, preventing grain growth, and material with an average particle size of 200 nm was obtained. It was determined that this material had a hardness value of 14.9 GPa and a toughness value of 3.8 MPa·m<sup>1/2</sup>. These results showed that the granular Y-TZP powders with amorphous structure obtained with the USP system provided an advantage in grain growth prevention in the sintering process through the HFIH system. According to the results of this study, grain growth, which is an important problem in the production of Y-TZP ceramics, was successfully prevented by rapid sintering processes.

## Acknowledgement

The authors would like to thank Kütahya Dumlupınar University and Advanced Technologies Center (İLTEM) for their support in the analysis.

## References

- [1] J. Li, J. Peng, S. Guo, L. Zhang, Application of response surface methodology (RSM) for optimization of the sintering process of preparation calcia partially stabilized zirconia (CaO-PSZ) using natural baddeleyite, *J. Alloys Compd.* 574 (2013) 504–511.
- [2] G. Rauchs, T. Fett, D. Munz, R. Oberacker, Tetragonal-to-monoclinic phase transformation in CeO<sub>2</sub>-stabilized zirconia under multiaxial loading, *J. Eur. Ceram. Soc.* 22 (2002) 841–849.
- [3] Y. Zhao, Y. Gao, Structural evolution of plasma-sprayed nanoscale 3 mol% and 5 mol% yttria-stabilized zirconia coatings during sintering, *Appl. Surf. Sci.* 425 (2017) 1033–1039.
- [4] L. Hao, D.R. Ma, J. Lawrence, X. Zhu, Enhancing osteoblast functions on a magnesia partially stabilised zirconia bioceramic by means of laser irradiation, *Mater. Sci. Eng. C* 25 (2005) 496–502.
- [5] M. Trunec, Z. Chlup, Higher fracture toughness of tetragonal zirconia ceramics through nanocrystalline structure, *Scr. Mater.* 61 (2009) 56–59.
- [6] F. Wakai, S. Sakaguchi, Y. Matsuno, Superplasticity of Yttria-Stabilized Tetragonal ZrO<sub>2</sub> Polycrystals, *Advanced Ceramic Materials 1* (1986) 259–263.
- [7] A. Bravo-Leon, Y. Morikawa, M. Kawahara, M.J. Mayo, Fracture toughness of nanocrystalline tetragonal zirconia with low yttria content, *Acta Mater.* 50 (2002) 4555–4562.
- [8] T. Okamoto, K. Yasuda, T. Shiota, Grain motion statistics of polycrystalline zirconia during superplastic deformation, *Scr. Mater.* 64 (2011) 253–255.
- [9] Y. Ye, J. Li, H. Zhou, J. Chen, Microstructure and mechanical properties of yttria-stabilized ZrO<sub>2</sub>/Al<sub>2</sub>O<sub>3</sub> nanocomposite ceramics, *Ceram. Int.* 34 (2008) 1797–1803.
- [10] A.S. Gandhi, V. Jayaram, A.H. Chokshi, Dense Amorphous Zirconia – Alumina by Low-Temperature Consolidation of Spray-Pyrolyzed Powders, *J. Am. Ceram. Soc.* 82 (1999) 2613–2618.
- [11] L. Gan, Y. Park, H. Kim, J. Kim, J. Ko, J. Lee, Journal of the European Ceramic Society Fabrication and microstructure of hot pressed laminated Y<sub>2</sub>O<sub>3</sub>/Nd:Y<sub>2</sub>O<sub>3</sub>/Y<sub>2</sub>O<sub>3</sub> transparent ceramics, *Journal of the European Ceramic Society Volume 36*, (2016) 911–916.
- [12] R. Poyato, J. Macías-Delgado, A. García-Valenzuela, R.L. González-Romero, A. Muñoz, A. Domínguez-Rodríguez, Electrical properties of reduced 3YTZP ceramics consolidated by spark plasma sintering, *Ceram. Int.* 42 (2016) 6713–6719.
- [13] C. Ergun, Enhanced phase stability in hydroxylapatite/zirconia composites with hot isostatic pressing, *Ceram. Int.* 37 (2011) 935–942.
- [14] A. Gionea, E. Andronescu, G. Voicu, C. Bleotu, V.A. Surdu, Influence of hot isostatic pressing on ZrO<sub>2</sub>-CaO dental ceramics properties, *Int. J. Pharm.* 510 (2016) 439–448.
- [15] K.A. Khalil, S.W. Kim, Mechanical wet-milling and subsequent consolidation of ultra-fine Al<sub>2</sub>O<sub>3</sub>-(ZrO<sub>2</sub>+3%Y<sub>2</sub>O<sub>3</sub>) bioceramics by using high-frequency induction heat sintering, *Trans. Nonferrous Met. Soc. China.* 17 (2007) 21–26.
- [16] S.W. Kim, S.L. Cockcroft, K.A. Khalil, K. Ogi, Sintering behavior of ultra-fine Al<sub>2</sub>O<sub>3</sub>-(ZrO<sub>2</sub>+Xmol% Y<sub>2</sub>O<sub>3</sub>)

- ceramics by high-frequency induction heating, *Mater. Sci. Eng. A*. 527 (2010) 4926–4931.
- [17] S.W. Kim, K.A. Khalil, S.L. Cockcroft, D. Hui, J.H. Lee, Sintering behavior and mechanical properties of HA-X% mol 3YSZ composites sintered by high frequency induction heated sintering, *Compos. Part B Eng.* 45 (2013) 1689–1693.
- [18] I.J. Shon, I.K. Jeong, J.H. Park, B.R. Kim, K.T. Lee, Effect of Fe<sub>2</sub>O<sub>3</sub> addition on consolidation and properties of 8 mol% yttria-stabilized zirconia by high-frequency induction heated sintering (HFIHS), *Ceram. Int.* 35 (2009) 363–368.
- [19] M. Gaudon, E. Djurado, N.H. Menzler, Morphology and sintering behaviour of yttria stabilised zirconia (8-YSZ) powders synthesised by spray pyrolysis, *Ceram. Int.* 30 (2004) 2295–2303.
- [20] M. Chen, J. He, Y. Zhang, Z. Ding, J. Luo, Densification and grain growth behaviour of high-purity MgO ceramics by hot-pressing, *Ceram. Int.* 43 (2017) 1775–1780.
- [21] Z. He, J. Ma, Grain-growth rate constant of hot-pressed alumina ceramics, *Mater. Lett.* 44 (2000) 14–18.
- [22] A.S. Gandhi, V. Jayaram, A.H. Chokshi, Low temperature densification behaviour of metastable phases in ZrO<sub>2</sub>-Al<sub>2</sub>O<sub>3</sub> powders produced by spray pyrolysis, *Mater. Sci.* 306 (2001) 785–789.
- [23] K. Matsui, H. Yoshida, Y. Ikuhara, Phase-transformation and grain-growth kinetics in yttria-stabilized tetragonal zirconia polycrystal doped with a small amount of alumina, *J. Eur. Ceram. Soc.* 30 (2010) 1679–1690.
- [24] S. Tekeli, Influence of alumina addition on grain growth and room temperature mechanical properties of 8YSCZ/Al<sub>2</sub>O<sub>3</sub> composites, *Compos. Sci. Technol.* 65 (2005) 967–972.
- [25] Y.W. Hsu, K.H. Yang, K.M. Chang, S.W. Yeh, M.C. Wang, Synthesis and crystallization behavior of 3 mol% yttria stabilized tetragonal zirconia polycrystals (3Y-TZP) nanosized powders prepared using a simple co-precipitation process, *J. Alloys Compd.* 509 (2011) 6864–6870.
- [26] R. Dwivedi, A. Maurya, A. Verma, R. Prasad, K.S. Bartwal, Microwave assisted sol-gel synthesis of tetragonal zirconia nanoparticles, *J. Alloys Compd.* 509 (2011) 6848–6851.
- [27] Y.N. Ko, S.M. Lee, J.H. Kim, J. Lee, Y.C. Kang, Processing Research Sintering characteristics of nano-sized yttria-stabilized zirconia powders prepared by spray pyrolysis, *J. Ceram. Process. Res.* 13 (2012) 405–408.
- [28] M. Koç, Synthesis and Characterization of Nanostructured Y-TZP-Al<sub>2</sub>O<sub>3</sub> Granule Composite Microspheres, PhD thesis, Kütahya Dumlupınar University Institute of Science, Kütahya, (2018) 152s.
- [29] M. Perez-Page, R. Guzalowski, D.N.F. Mucbe, R.H.R. Castro, P. Stroeve, Synthesis of porous yttria-stabilized zirconia microspheres by ultrasonic spray pyrolysis, *Mater. Lett.* 188 (2017) 41–44.
- [30] A. Nastic, A. Merati, M. Bielawski, M. Bolduc, O. Fakolujo, M. Nganbe, Instrumented and Vickers Indentation for the Characterization of Stiffness, Hardness and Toughness of Zirconia Toughened Al<sub>2</sub>O<sub>3</sub> and SiC Armor, *J. Mater. Sci. Technol.* 31 (2015) 773–783.
- [31] J. Lubauer, F. H., Schuenemann, R., Belli, U., Lohbauer, Speed- sintering and the mechanical properties of 3–5 mol% Y<sub>2</sub>O<sub>3</sub>- stabilized zirconias, *Odontology* (2023) 1-8.